NANO LETTERS

pubs.acs.org/NanoLett

Detuned Electrical Dipoles for Plasmonic Sensing

Andrey B. Evlyukhin,[†,‡] Sergey I. Bozhevolnyi,[*,†] Anders Pors,[§] Michael G. Nielsen,[†] Ilya P. Radko,[†] Morten Willatzen,[§] and Ole Albrektsen[†]

[†]Institute of Sensors, Signals and Electrotechnics (SENSE), University of Southern Denmark, Niels Bohrs Allé 1E, DK-5230 Odense M, Denmark, , [‡]Laser Zentrum Hannover e.V., Hollerithallee 8, D-30419 Hannover, Germany, and [§]Mads Clausen Institute (MCI), University of Southern Denmark, Alsion 2, DK-6400 Sønderborg, Denmark

ABSTRACT We demonstrate that a pair of electrical dipolar scatterers resonating at different frequencies, i.e., detuned electrical dipoles, can be advantageously employed for plasmonic sensing of the environment, both as an individual subwavelength-sized sensor and as a unit cell of a periodic array. It is shown that the usage of the ratio between the powers of light scattered into opposite directions (or into different diffraction orders), which peaks at the intermediate frequency, allows one to reach a sensitivity of ≈400 nm/RIU with record high levels of figure of merit exceeding 200. Qualitative considerations are supported with detailed simulations and proof-of-principle experiments using lithographically fabricated gold nanorods with resonances at ∼800 nm.

KEYWORDS Plasmonics, localized surface plasmons, plasmonic sensing

Recent devlopments have greatly improved the sensitivity of optical sensors that are based on metal nanoparticle (NP) arrays and individual NPs and exploiting localized surface plasmon resonances (LSPRs) associated with the resonant excitation of collective electron oscillations in metal NPs.[1] The LSRP wavelength is determined by the susceptibilities of constituent materials as well as by the NP size and geometry. The former feature provides the possibility of monitoring environmental changes by tracking the LSPR wavelength, whereas the latter allows one to adjust the LSPR position across the visible and near-infrared spectral regions. In this approach, the sensitivity (nm/RIU) is defined as the shift in the resonance wavelength per unit change of refractive index, with the overall performance being characterized by the "figure of merit" (FOM) that represents the sensitivity value divided by the resonance spectral width at half-maximum.[2] Both characteristics are rather difficult to improve, especially for single NP configurations.[1,3] For example, the LSPR quality (Q) factor is problematic to increase over the electrostatic limit imposed by the Ohmic losses in metals.[4] In fact, one can reach this limit only with *ultrasmall* metal NPs, whose scattering (radiation) losses are negligibly small with respect to the absorption losses. On the other hand, environmental sensing relies on the detection of scattered light so that, for practical purposes, NPs have to be chosen large enough to obtain measurable signals. Very recently several approaches, that enable controlling the radiation loss and thereby improving Q factors and the overall sensing performance, have been suggested, including the usage of complex plasmonic structures exhibiting Fano resonances[5] and electromagnetically induced transparency (EIT).[6]

In this Letter, we demonstrate that a pair of electrical dipolar scatterers resonating at different frequencies, i.e., detuned electrical dipoles (DED), can be advantageously employed for plasmonic sensing of environment, both as an individual subwavelength-sized sensor and as a unit cell of a periodic array. It is shown that the usage of the ratio between the powers of light scattered into opposite directions (or into different diffraction orders), which peaks at the intermediate frequency, allows one to reach a sensitivity of ∼400 nm/RIU with record high levels of figure of merit exceeding 200. Qualitative arguments are supported with detailed simulations and proof-of-principle experiments using lithographically fabricated gold nanorods with LSPRs in the near-infrared.

Our idea can be illustrated by considering two closely located *noninteracting* electric dipolar scatterers, whose resonances are equally detuned from the central frequency ω_0 so that their dipole polarizabilities can be represented as

$$\alpha_{1(2)}(\omega) = \frac{A{\omega_0}^2}{(\omega_0 \pm \delta)^2 - \omega^2 - i\Gamma\omega} \qquad (1)$$

where δ is the detuning frequency, Γ is the damping factor, and A characterizes their strength. This type of polarizability can readily be implemented in plasmonics for optical frequencies, e.g., with metal (gold or silver) NPs whose resonances can be adjusted by tuning their aspect ratios.[7] For weak detuning ($\omega_0 \gg \delta$), these polarizabilities at the central frequency read

* To whom correspondence should be addressed, seib@sense.sdu.dk.
Received for review: 07/22/2010
Published on Web: 09/29/2010

DOI: 10.1021/nl102572q | *Nano Lett.* **2010,** *10,* 4571–4577

$$\alpha_{1(2)}(\omega = \omega_0) \simeq \frac{A\omega_0(\pm 2\delta + i\Gamma)}{4\delta^2 + \Gamma^2} \quad (2)$$

implying that, upon uniform illumination at the central frequency, the scattered fields have different phases so that the total scattering can be strongly suppressed due to destructive interference. This suppression of scattering represents an optical analogue of the classical EIT in atomic systems considered using the dressed-state picture.[8] There is however a subtle difference that becomes *crucial* when the light incidence is perpendicular to the line connecting two scatterers. Since the scatterers are separated by a nonzero distance, d (Figure 1a), and the difference in phases $\Delta\Phi$ of two polarizabilities does not reach π in the presence of damping (eq 2)

$$\Delta\Phi(\omega_0) = (\Phi_2 - \Phi_1)_{\omega=\omega_0} = \pi - 2\arctan(\Gamma/2\delta) \quad (3)$$

the radiation scattering (at the central frequency) along the line connecting two scatterers is *strongly asymmetric*: the retardation phase due to the light propagation, kd (k is the wavenumber in the surrounding medium), can compensate the above phase difference in one direction of propagation (pointing from the "blue" scatterer resonating at a higher frequency $\omega_0 + \delta$ to the "red" one) and add up in the opposite direction, thereby enhancing and attenuating the (constructive) interference in the corresponding directions. The *main idea* of our approach is to take advantage of the DED scattering asymmetry for environmental sensing by monitoring the wavelength at which the ratio between the powers of light scattered in the *opposite* directions along the line connecting two scatterers is maximized.

It is clear that the strong-to-weak power ratio can be very large provided that the attenuation (in the red−blue direction) is complete, i.e., when $\Delta\Phi + kd = \pi$ or, alternatively

$$\tan(0.5kd) = 0.5\Gamma/\delta \quad (4)$$

The above condition can be satisfied for any DED pair by properly choosing their separation d. One can also require that the scattering in the opposite direction is maximized, which is achieved when the phase difference (eq 3) is completely compensated: $\Delta\Phi = kd$. It is thereby seen that the scattering *asymmetry* is maximized when the retardation phase, kd, and the phase difference, $\Delta\Phi$, are both equal to $\pi/2$, resulting in the following *optimal* conditions

$$d = \lambda_0/4n \quad \text{and} \quad \Gamma = 2\delta \quad (5)$$

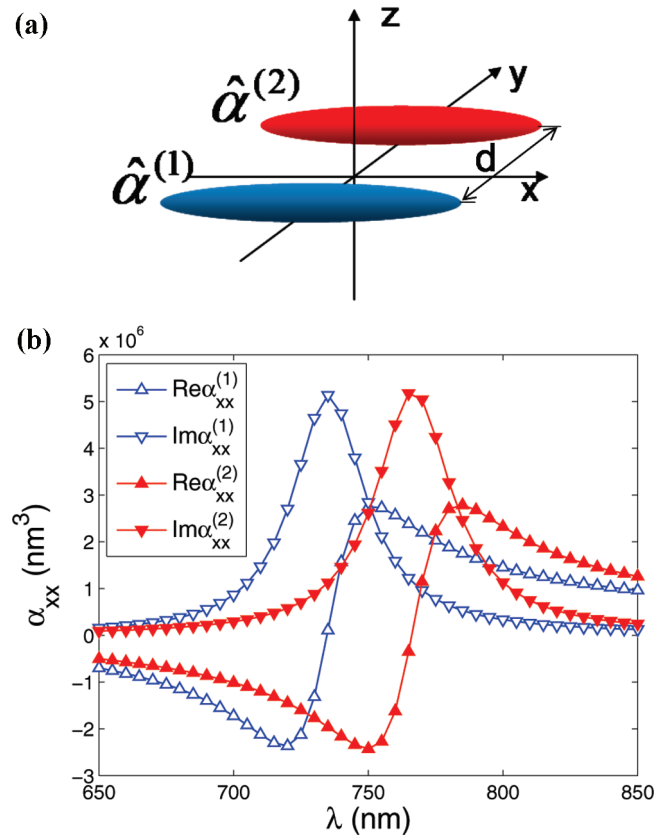

FIGURE 1. (a) Geometry of the considered configuration. (b) Real and imaginary parts of the corresponding component of polarizabilities of individual gold ellipsoids embedded in a dielectric with the refractive index of 1.4 and having the sizes of 67.8 × 20.0 × 20.0 and 68.9 × 18.6 × 18.6 nm^3.

where λ_0 is the vacuum wavelength at the central frequency and n is the medium refractive index.

The above conditions (eq 5), which maximize the asymmetry of scattering (along the y axis) under the illumination with the properly polarized (along the x axis) light propagating (along the z axis) perpendicular to the line connecting the scatterers (Figure 1a), are strictly valid only for *noninteracting* scatterers. Their interaction introduces, as will be seen below, small corrections (due to their relatively large separation), which can, in principle, also be taken into account. On the other hand, these corrections become less important and can be disregarded when considering the practical realization that introduces other uncertainties (e.g., due to fabrication inaccuracies).

Our approach is further demonstrated with the DED configuration consisting of two ellipsoid gold NPs embedded in a dielectric with the refractive index $n = 1.4$, separated by the distance $d = 134$ nm and exhibiting LSPRs at the wavelengths detuned equally from the wavelength of 750 nm (Figure 1), so that the optimal conditions (eq 5) are approximately satisfied. The scattering cross sections of individual NPs and that of the NP pair calculated self-consistently[9] using the tabular gold constants[10] show the

DOI: 10.1021/nl102572q | *Nano Lett.* **2010,** *10,* 4571–4577

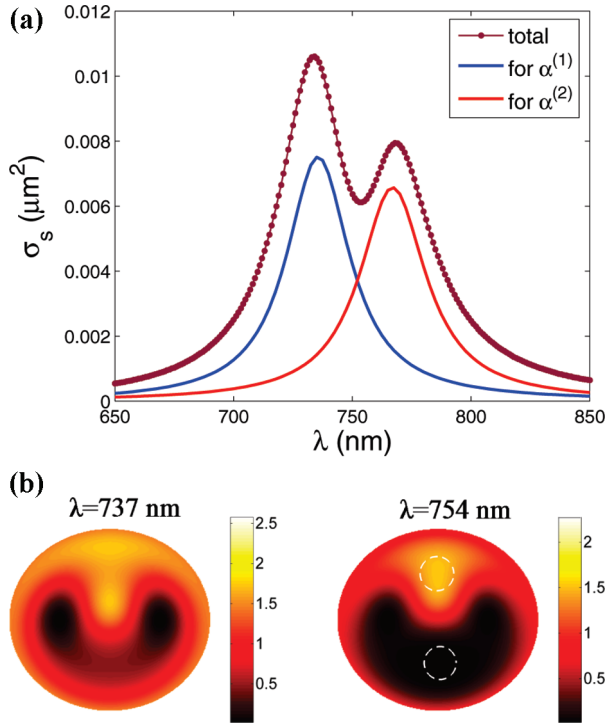

FIGURE 2. (a) Scattering spectra of individual NPs and NP pair. (b) Differential scattering cross sections ($\times 10^{-3}$ μm^2/sr) calculated for the incident x-polarized light propagating along the z axis at different wavelengths and displayed in spherical coordinates corresponding to the coordinate system shown in Figure 1a: the polar angle θ measured from the z axis is represented here by the radial distance, whereas the azimuthal angle ϕ counted in the xy plane from the x axis is displayed here in the figure plane with the x axis being horizontal. Two circles positioned at $\theta = \pi/2$ and $\phi = \pm\pi/2$ mark the integration areas used for calculations shown in Figure 3.

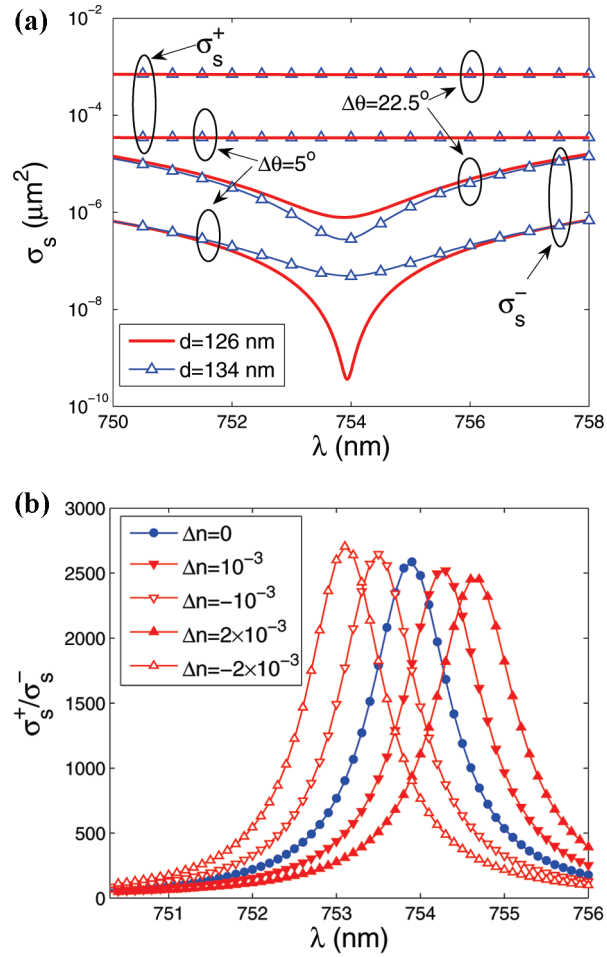

FIGURE 3. (a) Spectra of the cross sections of scattering into the directions of constructive (σ_s^+) and destructive (σ_s^-) interference calculated for the incident x polarized light propagating along the z axis (Figure 1a) for two DED separations and two solid angles. (b) Spectra of the ratio between the scattering cross sections calculated for $d = 134$ nm with the cone angle $\Delta\theta = 22.5°$ for different dielectric environment: $n = 1.4 + \Delta n$. The solid angles are indicated by dashed circles in Figure 2b.

expected EIT-like behavior that also reflects the influence of coupling (Figure 2a).

Angular distributions of the differential scattering cross section of the NP pair shown at the "blue" resonance wavelength of 737 nm and at the DED wavelength of 754 nm demonstrate the effect of remarkably strong asymmetry in the NP scattering at the DED wavelength (Figure 2b). Asymmetry in the scattering pattern is also noticeable at the wavelength of 737 nm because the contribution from (relatively weak at this wavelength) "red" scatterer interferes along the y axis either in or out of phase with that of "blue" scatterer. It should be noted that the DED wavelength (defined hereafter as the wavelength that minimizes the scattering of DED scatterers in the direction of their destructive interference) is slightly larger than the wavelength of 750 nm centered between the LSPRs of individual NPs (Figure 1b) due to their interaction. For the same reason, their separation ensuring the *complete* attenuation of scattering in the red−blue direction (at the DED wavelength of 754 nm) was found to be $d = 126$ nm, i.e., smaller than that obtained for noninteracting scatterers (eq 5).

For the practical realization of environmental sensing, we suggest measurements of a wavelength dependence of ratio between the powers of light scattered into oppositely oriented solid angles centered along the y axis (Figure 2b). The corresponding spectra of scattering cross sections were calculated (by integrating the differential cross sections) for two solid angles characterized with the cone angles $\Delta\theta = 5°$ and 22.5° and for two DED separations in real space, $d = 126$ and 134 nm (Figure 3a). It is seen that, while the nearly complete extinction is realized for $d = 126$ nm and $\Delta\theta = 5°$, the scattering cross sections (that determine the scattered powers) are considerably larger for $\Delta\theta = 22.5°$ with extinction being *stronger* for $d = 134$ nm, a DED separation that was found from the optimal conditions (eq 5). To give an example, for the latter configuration ($d = 134$ nm, $\Delta\theta = 22.5°$) illuminated with the intensity of 1 mW/μm^2, the scattered powers at the DED wavelength would amount to $P^+ \simeq 0.7$ μW and $P^- \simeq 0.3$nW that should be possible to reliably detect. The wavelength dependence of the power ratio exhibits thereby an extremely sharp maxi-

DOI: 10.1021/nl102572q | Nano Lett. 2010, 10, 4571–4577

mum (≃2500) at the DED wavelength, which is dictated by the refractive index of dielectric environment (Figure 3b). The peak position is found to shift linearly with the change in the dielectric refractive index, showing the sensitivity (peak shift per unit change of refractive index) of ≈400 nm/RIU, which is a typical value for LSPR-based sensors.[1] The corresponding FOM defined as the sensitivity value divided by the full width at half-maximum (fwhm) of resonance peak[2] was found to reach a record high value of ≃300. It should be borne in mind that, in practice, the fwhm and thereby FOM deteriorate rapidly in the presence of noise in measurements. For example, we found that adding to the calculated scattering spectra (Figure 3) a constant (noise) contribution at the level of scattering in the direction of destructive interference (at the DED wavelength) results in a decrease of the peak power ratio from ≃2600 to 1300 and increase of the fwhm from ≃1.3 to 1.8 nm. However, even in this case, the FOM would still be reaching a very high level of ≃220, indicating the robustness of the suggested DED-based approach.

The scattered power available for the detection can be significantly increased if the same idea is implemented using a periodic array of DED pairs (Figure 4a). In this case, the scattering directions with constructive and destructive interference can be chosen to coincide with the directions of light diffraction into ±first orders. The corresponding retardation phase should, in this case, be considered in the direction of light diffraction determined by the array period Λ_y along the line connecting DED scatterers. The retardation phase kd in the above relations (eqs 4 and 5) should therefore be changed onto $kd \sin\theta$, where θ is the diffraction angle given by the grating equation: $\sin\theta = \lambda/(n\Lambda_y)$. This modification results in the following conditions required to extinguish one and maximize another diffraction order (see eq 5)

$$d = \Lambda_y/4 \quad \text{and} \quad \Gamma = 2\delta \tag{6}$$

which are again strictly valid only for noninteracting scatterers. The periodicity in the other direction, Λ_x, should be as small as possible to increase the density of DED pairs but large enough so as to not result in the strong coupling between the neighbor DED pairs.

In our numerical example, we have used the same gold ellipsoids as above (Figure 1) arranged in a two-dimensional array ($\Lambda_x = 400$ and $\Lambda_y = 800$ nm) but separated with the center-to-center distance $d = 200$ nm (Figure 4a) in order to comply with the optimal conditions for DED arrays (eq 6). An increase of the DED separation from 134 to 200 nm led to a decrease in the DED interaction, causing the DED wavelength, 752 nm (Figure 4b), to be closer to that of noninteracting scatterers, 750 nm (Figure 1b), as compared to the previous case, 754 nm (Figure 3a). The far-field angular distributions of the scattered power calculated for the DED array of 8 × 8 μm^2 illuminated with a Gaussian

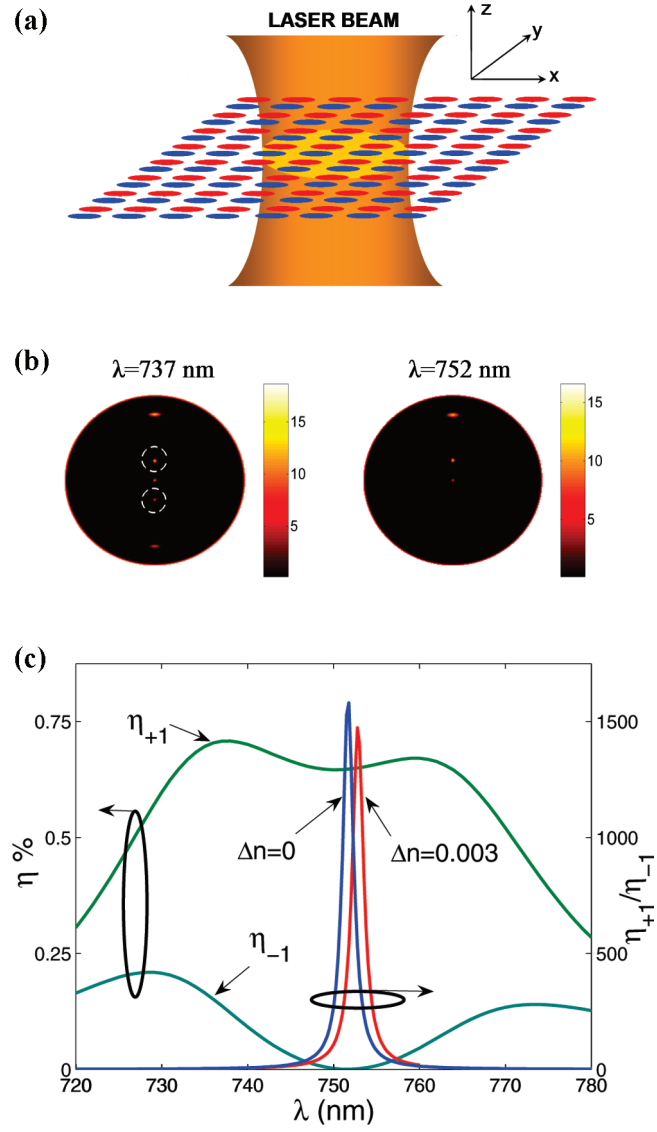

FIGURE 4. (a) Schematic representation of a laser beam (waist ≃3 μm) incident on an array ($\Lambda_x = 400$ and $\Lambda_y = 800$ nm) of DED pairs ($d = 200$ nm) of the considered gold ellipsoids (Figure 1) embedded in a dielectric ($n = 1.4$). (b) Far-field angular distributions of scattered power (arbitrary units) calculated at different wavelengths. Dashed circles indicate the positions of the ±first diffraction orders in the forward direction. (c) Wavelength dependencies of the corresponding diffraction efficiencies, η, and their ratio calculated for different dielectric environments ($n = 1.4 + \Delta n$) by integrating the scattered power within dashed circles shown in (b).

beam (waist ≃3 μm) of x-polarized radiation show, along the y axis, the ±first diffraction orders in the forward (circled) and backward directions, whose intensities strongly depend on the wavelength (Figure 4b). Wavelength dependencies of the diffraction efficiencies in the forward direction exhibit a very strong scattering asymmetry similar to that found for an individual DED pair (Figure 3a). The ratio between the diffraction efficiencies features correspondingly a very strong and narrow peak whose position shifts proportionally to a change in the refractive index (Figure 4c), indicating the same levels of sensitivity (≈400 nm/RIU) and FOM (≃250)

DOI: 10.1021/nl102572q | Nano Lett. 2010, 10, 4571–4577

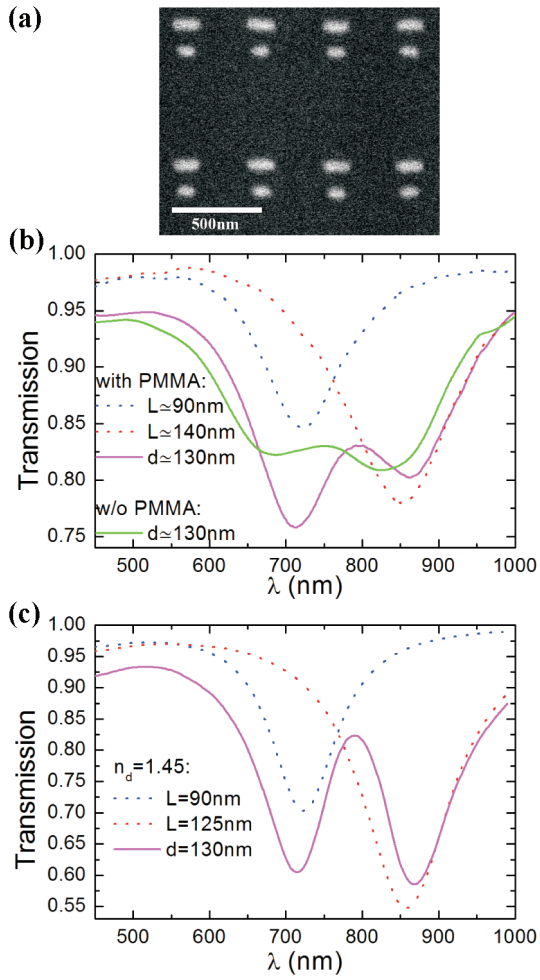

FIGURE 5. (a) Electron microscopy image of the fabricated array (Λ_x = 400 and Λ_y = 750 nm) of gold nanorods being ≃50 × 50 nm² in the cross section with the lengths of ≃90 and 140 nm and the center-to-center distance of ≃130 nm. (b) Transmission spectra measured for the array of nanorod pairs (solid lines) before and after the deposition of a PMMA layer along with the spectra of arrays of the individual nanorods (dotted lines). (c) Theoretically calculated spectra of arrays of individual (dotted lines) and paired (solid line) nanorods (≃50 × 50 nm² in cross section with the lengths of ∼90 and 125 nm) embedded in dielectric with the refractive index of 1.45.

as those found above for an individual DED pair (Figure 3b). The main advantage of using DED arrays instead of an individual DED pair is thereby in the possibility to significantly increase the radiation power available for the detection, since the strongest signals can reach the level of 1 % of the incident power (Figure 4c).

For proof-of-principle experiments, we fabricated periodic (Λ_x = 400 and Λ_y = 750 nm) arrays (50 × 50 μm²) consisting of individual and double gold nanorods (of different lengths) on a silica substrate using electron-beam lithography and lift-off applied to a 50 nm thick gold film (Figure 5a). Transmission spectra were measured using a broad band halogen light source with a fiber output whose (weakly divergent) radiation was directed (at normal incidence) through a polarizer on the fabricated arrays of nanorods aligned so that their axes were parallel to the light polarization. The transmitted radiation was collected with an objective and fed into an optical fiber connected to a spectrometer. The transmission spectra were measured before and after depositing a thick (several micrometers) layer of poly(methyl methacrylate), i.e., PMMA. The latter was used to form a homogeneous dielectric environment for gold nanorods. The transmission spectra obtained with arrays of nanorod pairs before and after the deposition of the PMMA layer feature local maxima located at ∼755 and 790 nm, respectively, each being surrounded by two local minima (Figure 5b). These maxima indicate the suppression of scattering achieved at the wavelengths that are intermediate with respect to the resonance wavelengths of individual nanorods, a phenomenon that is akin to the classical EIT in atomic systems considered using the dressed-state picture[8] as discussed earlier. The effect of enhanced transmission is especially pronounced and documented in detail for the arrays covered with the PMMA layer: the transmission spectra obtained with the arrays of individual short and long nanorods exhibit the effect of detuning in their resonances located at ≃720 and 860 nm, while the transmission spectrum of the array consisting of pairs of corresponding nanorods (Figure 5a) shows the effect of increased transmission at the intermediate wavelength of ≃790 nm (Figure 5b). Note also a significant red shift in the transmission spectrum of the DED array after the deposition of the PMMA layer (due to a change in the dielectric environment of nanorods), as well as an improvement in the contrast. This improvement is related to the nature of plasmon resonances in gold nanorods: their resonances are determined by the interference of counterpropagating short-range surface plasmon polaritons reflected by the nanorod terminations.[11] Similarly to the case of metal nanowires,[12,13] the mode field confinement and effective index of these plasmon modes increase with an increase of the refractive index of surrounding dielectric medium resulting in a red shift of the standing-wave resonance that becomes also better pronounced in the case of a homogeneous dielectric environment.

We have attempted to model the response of fabricated arrays with the finite-element method (FEM) implemented in the commercial software COMSOL. Individual and double gold nanorods being ≃50 × 50 nm² in the cross section with the lengths of ≃90 and 125 nm and the center-to-center distance of ≃130 nm were considered to be embedded in dielectric with the refractive index of 1.45. Transmission spectra were then calculated using their computed extinction cross sections and the corresponding size (400 × 750 nm²) of unit cell (Figure 5c). It is seen that the positions of local minima and maximum in the transmission spectra correspond well to the experimental results (Figure 5b), albeit for a slightly shorter length of the long nanorod, but the contrast obtained in simulations is much better than that achieved in the experiment. It should be borne in mind that the use of divergent illumination and detection of focused

DOI: 10.1021/nl102572q | *Nano Lett.* **2010,** *10,* 4571–4577

radiation as well as inhomogenous broadening (due to fabrication-induced deviations of nanorod dimensions in the fabricated arrays) could definitely contribute to smearing out the spectral features in these *preliminary* experiments.

The fabricated DED array (Figure 5a) covered with the PMMA layer was further characterized in the setup for leakage-radiation microscopy (LRM)[14] using a continuous-wave-operated tunable Ti:sapphire laser, whose radiation polarized parallel to the nanorod axes was slightly focused and directed at normal incidence on the sample (Figure 6a) with the incident light powers being on the level of a few milliwatts. The ±first diffraction orders observed in the back focal plane of an LRM objective exhibited strong asymmetry (Figure 6b) in their wavelength-dependent behavior as expected (cf. Figure 4b). Wavelength dependencies of the corresponding diffraction efficiencies measured with a calibrated photodetector resulted in a very sharp peak of their ratio at the wavelength of ≃785 nm with the fwhm of ≃20 nm (Figure 6c), a value which is *significantly* smaller than the fwhm of plasmonic resonances for individual nanorods (Figure 5b). Such a drastic narrowing of the system response at resonance constitutes the main *forte* of the DED-based plasmonic nanostructures. Since the sensitivity (nm/RIU) of plasmonic resonances is difficult to appreciably increase, the FOM can radically be increased only by narrowing the resonance line width.[1] Note that the fabricated and characterized DED array was not optimized with respect to the nanorod parameters and their separation, resulting in a significantly smaller maximum ratio as compared to the model case (Figure 4c). The balance between the strengths, resonance positions, and spatial separation of individual nanorods (that should also be related to the array periodicity) is quite delicate: one should achieve the *same* scattering strength of interacting DED scatterers *simultaneously* with fulfilling the optimum conditions (eq 6) in order to ensure the highest ratio between the diffraction efficiencies. Still, the effect of destructive interference of DED pairs is rather robust as demonstrated with our *proof-of-principle* experiments (Figure 6b,c). It should be mentioned that we characterized also similar arrays of DED pairs with a smaller center-to-center separation (≃100 nm) and found a similarly sharp system response with the maximum ratio (between the diffraction efficiencies) of ≃40 and the fwhm of ≃30 nm. Finally, assuming that the sensitivity of the fabricated array is on the same level as that obtained in our simulations, i.e., ≃ 400 nm/RIU, one obtains the FOM of ≃20, a value which is very close to the record one obtained with ordered arrays of nanoholes in gold fabricated by soft interference lithography.[15]

In conclusion, it has been shown that a pair of electrical dipolar scatterers resonating at different frequencies, i.e., detuned electrical dipoles (DED), can be advantageously employed for plasmonic sensing of environment, both as an individual subwavelength-sized sensor and as a unit cell of a periodic array. It has been demonstrated that the usage of

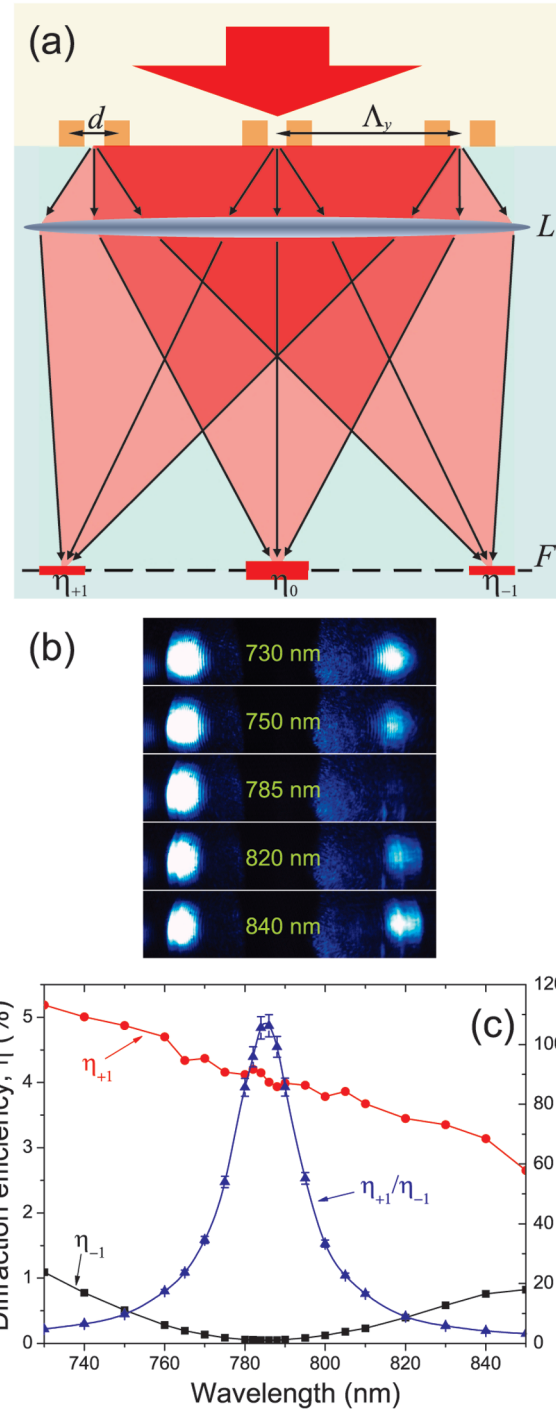

FIGURE 6. (a) Experimental leakage-radiation microscopy configuration used to detect radiation diffracted by the DED array shown in Figure 5a) after the deposition of the PMMA layer. Lens *L* denotes a high-numerical-aperture objective (N.A. = 1.25). The back focal plane *F* of the objective represents the location of a Fourier-transformed image of the radiation emerging from the sample. (b) Images taken in the Fourier plane *F* with the sample being illuminated at different wavelengths. The left and right spots correspond to the ±first diffraction orders with the (brightest) zeroth diffraction order being blocked to enhance the contrast of images. (c) Wavelength dependencies of the corresponding diffraction efficiencies, *η*, together with their ratio.

the ratio between the powers of light scattered into opposite directions (or into different diffraction orders), which peaks

DOI: 10.1021/nl102572q | *Nano Lett.* **2010,** *10,* 4571–4577

at the intermediate frequency, allows one to reach a sensitivity of ≈400 nm/RIU with record high levels of figure of merit exceeding 200. Qualitative considerations were supported with detailed simulations and proof-of-principle experiments using lithographically fabricated gold nanorods with resonances at ∼800 nm. We have experimentally demonstrated a *dramatic* narrowing of the system response at resonance, achieving the fwhm of ≃20 nm with gold nanorods in the near-infrared, due to destructive interference of light scattered by DED scatterers. We believe that the results obtained demonstrate convincingly strong potential of this novel sensing approach for different applications, especially in chemical and biological investigations. Clearly, the DED-based plasmonic configurations can be implemented with different resonant nanoparticles,[16−20] opening a doorway to numerous applications in sensing and metamaterials at optical frequencies similarly to other recently explored approaches.[5,6] It should be emphasized that, in our approach, plasmonic scatterers resonate at *different* frequencies and, being placed relatively far away from each other, interact only *weakly* (their interaction is not even required), a circumstance that results in somewhat relaxed requirements to the precision in their fabrication. Finally, our planar design facilitates successive stacking of layers containing DED scatterers, allowing for further increase of the detected signals (for sensing applications) or fabrication of "slow light" devices using the effect of increased light transmission at the DED wavelength.

Acknowledgment. The authors acknowledge financial support of this work by the VELUX Foundation and the Danish Council for Independent Research (FTP Contract No. 09-072949).

REFERENCES AND NOTES

(1) Anker, J. N.; Hall, W. P.; Lyandres, O.; Shah, N. C.; Zhao, J.; Duyne, R. P. V. *Nat. Mater.* **2008**, *7*, 442–453.
(2) Sherry, L. J.; Chang, C.; Schatz, G. C.; Duyne, R. P. V. *Nano Lett.* **2005**, *5*, 2034–2038.
(3) Sherry, L. J.; Jin, R.; Mirkin, C. A.; Schatz, G. C.; Duyne, R. P. V. *Nano Lett.* **2006**, *6*, 2060–2065.
(4) Wang, F.; Shen, Y. R. *Phys. Rev. Lett.* **2006**, *97*, 206806.
(5) Verellen, N.; Sonnefraud, Y.; Sobhani, H.; Hao, F.; Moshchalkov, V. V.; Dorpe, P. V.; Norlander, P.; Maier, S. A. *Nano Lett.* **2009**, *9*, 1663–1667.
(6) Liu, N.; Weiss, T.; Mesch, M.; Langguth, L.; Eigenthaler, U.; Hirscher, M.; Sönnichsen, C.; Giessen, H. *Nano Lett.* **2010**, *10*, 1103–1107.
(7) Park, K.; Koerner, H.; Vaia, R. A. *Nano Lett.* **2010**, *10*, 1433–1439.
(8) Boller, K. J.; Imamoglu, A.; Harris, S. E. *Phys. Rev. Lett.* **1991**, *66*, 2593–2596.
(9) Evlyukhin, A. B.; Bozhevolniy, S. I. *Surf. Sci.* **2005**, *590*, 173–180.
(10) Johnson, P. B.; Christy, R. W. *Phys. Rev. B* **1972**, *6*, 4370–4379.
(11) Nielsen, M. G.; Pors, A.; Nielsen, R. B.; Boltasseva, A.; Albrektsen, O.; Bozhevolnyi, S. I. *Opt. Express* **2010**, *18*, 14802–14811.
(12) Ditlbacher, H.; Hohenau, A.; Wagner, D.; Kreibig, U.; Rogers, M.; Hofer, F.; Aussenegg, F. R.; Krenn, J. R. *Phys. Rev. Lett.* **2005**, *95*, 257403.
(13) Falk, A. L.; Koppens, F. H. L.; Yu, C. L.; Kang, K.; Snapp, N. L.; Akimov, A. V.; Jo, M.-H.; Lukin, M. D.; Park, H. *Nat. Phys.* **2009**, *5*, 475–479.
(14) Radko, I. P.; Evlyukhin, A. B.; Boltasseva, A.; Bozhevolnyi, S. I. *Opt. Express* **2008**, *16*, 3924–3930.
(15) Henzie, J.; Lee, M. H.; Odom, T. W. *Nat. Nanotechnol.* **2007**, *2*, 549–554.
(16) Acimovic, S. S.; Kreuzer, M. P.; González, M. U.; Quidant, R. *ACS Nano* **2009**, *3*, 1231–1237.
(17) Prashant, K. J.; El-Sayed, M. A. *Nano Lett.* **2008**, *8*, 4347–4352.
(18) Huang, X.; Neretina, S.; El-Sayed, M. A. *Adv. Mater.* **2009**, *21*, 4880–4910.
(19) Lassiter, J. B.; Knight, M. W.; Mirin, N. A.; Halas, N. J. *Nano Lett.* **2009**, *9*, 4326–4332.
(20) Bardhan, R.; Grady, N. K.; Cole, J. R.; Joshi, A.; Halas, N. J. *ACS Nano* **2009**, *3*, 744–752.

DOI: 10.1021/nl102572q | *Nano Lett.* **2010,** *10,* 4571–4577